



Available online at <http://scik.org>

Commun. Math. Biol. Neurosci. 2025, 2025:70

<https://doi.org/10.28919/cmbn/9131>

ISSN: 2052-2541

## COMPUTATIONAL ANALYSIS OF MOLECULAR DESCRIPTORS FOR ANTI-TUBERCULOSIS DRUGS USED IN TUBERCULOSIS TREATMENT THROUGH QUANTITATIVE STRUCTURE-PROPERTY RELATIONSHIPS

MUHAMMAD ABID<sup>1,\*</sup>, KASHIF ALI<sup>1</sup>, MUHAMMAD IMRAN QURESHI<sup>2</sup>, HAFEEZ SULTANA<sup>3</sup>,  
MOHAMED Z. SAYED-AHMED<sup>4,5,6</sup>

<sup>1</sup>Department of Mathematics, COMSATS University Islamabad, Lahore Campus, Lahore, Pakistan

<sup>2</sup>Department of Mathematics, COMSATS University Islamabad, Vehari Campus, Lahore, Pakistan

<sup>3</sup>Department of Mathematics, Faculty of Science, Jazan University, Jazan 45142, Saudi Arabia

<sup>4</sup>Pharmacy Practice Research Unit, Department of Clinical Practice, College of Pharmacy, Jazan University,  
Jazan, 45142, Saudi Arabia

<sup>5</sup>Department of Internal Medicine and Infectious Diseases, Faculty of Veterinary Medicine, Mansoura University,  
Mansoura 35516, Egypt

<sup>6</sup>Department of Clinical Practice, College of Pharmacy, Jazan University, Jazan, 45142, Saudi Arabia

Copyright © 2025 the author(s). This is an open access article distributed under the Creative Commons Attribution License, which permits unrestricted use, distribution, and reproduction in any medium, provided the original work is properly cited.

**Abstract.** Tuberculosis poses a major public health challenge due to its widespread prevalence and severe health impact, necessitating the development of effective therapeutic agents. This study analyzes the structural and physicochemical characteristics of 13 anti-tuberculosis drugs, including Isoniazid, Levofloxacin, and Bedaquiline, using distance-based topological descriptors, particularly the Mostar index. A computational approach involving the Mostar index and Quantitative Structure-Property Relationship (QSPR) analysis was employed to predict critical drug properties like melting point and molar mass. The findings revealed strong correlations (melting point  $R > 0.990$ , molar mass  $R > 0.970$ ), demonstrating the predictive potential of the Edge Mostar index. These results

---

\*Corresponding author

E-mail address: [rmabidmath002@gmail.com](mailto:rmabidmath002@gmail.com)

Received January 16, 2025

offer valuable insights into the structural properties of anti-tuberculosis drugs, supporting the development of novel agents by leveraging the Mostar index for improved drug design.

**Keywords:** mycobacterium; tuberculosis drugs; structural descriptors; QSPR analysis; regression models; correlation coefficients.

**2020 AMS Subject Classification:** 92C42.

## 1. INTRODUCTION

Tuberculosis (TB) is a contagious bacterial infection caused by *Mycobacterium tuberculosis*, primarily affecting the lungs, but it can also spread to other organs through the bloodstream. It is one of the top 10 causes of death worldwide, especially in low- and middle-income countries. TB spreads through airborne droplets when an infected person coughs, sneezes, or talks. Symptoms include a persistent cough, chest pain, fever, night sweats, and weight loss. The disease is particularly dangerous for immunocompromised individuals, such as those with HIV/AIDS. Treatment involves a combination of antibiotics over a long duration, typically six months, but drug-resistant strains pose significant challenges to TB control. Efforts such as early detection, vaccination (BCG), and improved public health strategies are crucial in curbing its spread. According to the World Health Organization, TB claimed 1.5 million lives in 2020, making it a persistent global health threat [1, 2].

The management of tuberculosis (TB) entails a regimen of multiple drugs, each serving a distinct function in suppressing the proliferation of *Mycobacterium tuberculosis*, the bacterium that causes TB. Isoniazid (S1) is a highly effective first-line medication that inhibits bacterial cell wall formation. Pyrazinamide (S2) and Ethionamide (S3) are essential in early treatment by impairing bacterial metabolism, particularly during the latent phase of tuberculosis [3, 4, 5]. Fluoroquinolones such as Levofloxacin (S4) and Ofloxacin (S6) impede bacterial DNA replication, whereas Amikacin (S5) and Kanamycin (S12), classified as aminoglycosides, function by obstructing protein synthesis in bacteria. These medications are crucial for cases of multidrug-resistant tuberculosis, in which the germs exhibit resistance to standard therapies [6, 7, 8, 19].

Additional second-line medications are essential for managing more intricate or drug-resistant tuberculosis cases. Cycloserine (S7) disrupts cell wall production, whereas 4-aminosalicylic acid (S8) functions as a bacteriostatic agent, impeding bacterial proliferation.

Ethambutol (S9) impedes cell wall synthesis and is frequently employed in combination therapy to avert resistance. Ciprofloxacin (S10), a fluoroquinolone, inhibits bacterial DNA gyrase, resulting in bacterial mortality [9, 10, 11]. Bedaquiline (S11) is a novel pharmaceutical agent designed for drug-resistant tuberculosis, functioning by obstructing ATP generation in the bacterium. Streptomycin (S13), an antiquated antibiotic, is predominantly utilized against more resistant types of tuberculosis, functioning by obstructing bacterial protein synthesis. The appropriate utilization of this drug combination is essential for the successful treatment of tuberculosis, especially in complex or resistant cases [12, 13, 14].

Topological indices are numerical values derived from the structural properties of molecular graphs and have found extensive applications in chemistry and materials science. They serve as essential tools in Quantitative Structure-Property Relationship (QSPR) and Quantitative Structure-Activity Relationship (QSAR) studies, enabling researchers to predict a wide range of physicochemical, biological, and pharmacological properties of chemical compounds without the need for exhaustive experimental testing. For instance, valency-based and spectrum-based descriptors have proven effective in predicting physical and pharmacological properties of polycyclic compounds, aiding in drug discovery and development [15, 16]. Moreover, topological indices such as distance-based entropy measures have been utilized to explore the structural characteristics of dendrimers, enhancing the understanding of their chemical behavior [17]. Additionally, newly introduced topological invariants have demonstrated significant correlations with the properties of polycyclic compounds, further broadening their applicability in chemical and mathematical studies [18].

Streptomycin, a well-known antibiotic used to combat bacterial infections, serves as an excellent candidate for topological analysis. By examining the molecular graph of Streptomycin through the lens of the Mostar and edge Mostar indices, we aim to uncover how the drug's structure correlates with its function. The Mostar index is determined by comparing the number of vertices closer to each endpoint of an edge, highlighting the local asymmetry within the graph. The edge Mostar index extends this concept, focusing specifically on the edge-based asymmetry.

During the year 1947, Harold Wiener made the initial suggestion for topological indices, which was subsequently mentioned in Wiener's work [20]. Over the course of the succeeding time period, he proceeded to publish a series of articles that shed light on the relationship between the Wiener index and the physicochemical properties of carbon-based compounds [21]. According to the reference [22], this decade of the 20th century saw the computation of a considerable number of topological indices that are connected to the Wiener index. These indices were computed during the final decade of the century. Researchers have been estimating irregularity topological indices for a variety of chemical structures [23] from the beginning of the 21st century and continuing to do so during the second decade of the century. A number of new Banhatti indices were introduced in the year 2016 by V. R. Kulli [24]. These new Banhatti indices included modified Banhatti indices, super K Banhatti indices, and K Banhatti indices.

A lot of people in the area of chemical graph theory have been interested in studying degree-based, irregular, and distance-based topological indices in the last ten years. These indices have recently attracted a lot of attention from researchers looking to better understand molecular structures. As an example, A. Fahad and M. I. Qureshi [25, 26] examined polynomials of Poly(ETHyleneAmidoAmine) (PETAA) dendrimers and eccentricity-based topological indices in 2019. Their research brought attention to novel methods for describing molecular graphs. In November 2020, A. Fahad further investigated the topological characteristics of PETIM dendrimers, contributing important information to this expanding area of study. In the same year, M. I. Qureshi shifted his attention to the Zagreb connection index, particularly as it pertained to chemical structures associated with drugs. Adding to our understanding of the behavior of these structures, Yu-Ming Chu continued to investigate topological indices in 2021 by computing irregular indices for specific metal-organic frameworks [27, 28].

Also, bond-additive topological descriptors are being used more and more to describe the features of chemical graphs and the parts that make them up. The Wiener index is a new bond-additive index that gives each bond an input based on the number of atoms on both sides. This gives a clear measure of how connected molecules are. Since this start, many better descriptors have been created, such as the Szeged, revised-Szeged, PI, irregularity, and Zagreb indices [29]. The Mostar index is a new bond-additive topological measure that was just released by Došlic

and his colleagues [30]. This index gives information about how peripheral certain bonds are, and then adds up their effects to make a full measure of peripherality in the chemical structure. Understanding the peripherality of bonds is important in chemistry because it has a big effect on predicting the physicochemical features of molecules, which in turn changes how they behave in different situations. Tratnik significantly advanced [32] by demonstrating that the Mostar index of a weighted graph may be determined by comparing it to the quotient graphs. This discovery simplified index calculation for complex-weighted structures. According to [33], Arockiaraj and his team accurately calculated the Mostar index for molecular shapes like carbon nanocones and coronoid structures. The exact numbers revealed new aspects of these unusual molecular configurations. Arockiaraj et al. extended on their work in [34] by determining weighted Mostar indices for molecular peripheral forms. These indices can be employed in graphene, graphyne, and graphdiyne nanoribbons. Došlic et al. calculated the edge Mostar index for benzenoid systems using the techniques outlined in [30]. They also found exceptional Mostar index values for trees and unicyclic networks. This improved their understanding of this index for more molecule forms. Later, [31] introduced formulas for bicyclic graph Mostar index. These extended graph analysis to more complex structures. In [35], Hayat and Zhou made a big addition by finding the extreme edge Mostar index values for cacti and structures that look like trees. They showed how mentioned index can be used to look at different types of molecular graphs and how extremal behavior works in both simple and complex structures.

Although the above literature review discusses extensive work related to the Mostar and Edge Mostar index, this research primarily focuses on its mathematical aspects. Mathematicians have extensively studied the mathematical properties of the Edge Mostar index, exploring its theoretical foundations and implications within pure mathematics. However, our work is the first to investigate the chemical applicability of the Edge Mostar index. We achieved this by performing a detailed sensitivity analysis to evaluate its behavior and subsequently conducting a QSPR (Quantitative Structure-Property Relationship) analysis to explore its relevance in chemical studies. The Mostar index of a graph  $G$  is defined as

$$(1) \quad Mo(G) = \sum_{uv \in E(G)} |n_u - n_v|$$

where  $n_u$  and  $n_v$  are the number of vertices of  $G$  closer to  $u$  than  $v$  and the number of vertices of  $G$  closer to  $v$  than  $u$  respectively. The edge version of mostar index is defined as

$$(2) \quad Mo_e(G) = \sum_{e=uv \in E(G)} |m_u - m_v|$$

where  $m_u$  and  $m_v$  are the number of edges of  $G$  closer to  $u$  than  $v$  and the number of edges of  $G$  closer to  $v$  than  $u$  respectively.

In this paper, we derive explicit formulas for both indices as applied to Streptomycin and discuss their implications in terms of molecular structure and drug activity, but before this, we analyzed the implacability of these descriptors by applying Smoothness, Abruptness and QSPR regression analysis. This analysis contributes to the broader application of topological indices in pharmaceutical chemistry, providing insights that may assist in the development of more effective drugs. In our work, Matlab is utilized for mathematical calculations and verifications whereas Maple is used for graphically analyzing and plotting these results and ChemSketch is used to draw the molecular graphs.

## 2. STRUCTURE-SENSITIVITY ANALYSIS

Several parameters were introduced to reduce randomness in constructing a new topological index. One key parameter is smoothness, which ensures a molecular descriptor's value changes uniformly with gradual structural changes [36, 37, 38]. However, assessing smoothness is challenging and often overlooked by researchers. This section explores the smoothness of some novel degree-based topological indices and compares them with existing results. Two graph structural measures, denoted as structural sensitivity ( $\Psi_s$ ) and abruptness ( $\Delta_a$ ), were proposed to evaluate smoothness. The structural sensitivity of eigenvalue-based indices and the smoothness of graph energy in chemical graphs have been studied. An existing algorithm for calculating  $\Psi_s$  and  $\Delta_a$  is also outlined.

### (1) Initialize Variables:

- Matrices for trees, GED, topological indices, and results are initialized.
- Tree set  $\Omega$  and GED for all trees are computed using a Python package.

### (2) Calculate TIs for Each Tree:

- Loop through each tree  $T_i$  in the dataset.

- Compute structure sensitivity  $\Psi_s(T_i, \text{TIs})$  and abruptness  $\Delta_a(T_i, \text{TIs})$  for each TI.
- Store all  $\Psi_s$  and  $\Delta_a$  values for each tree.

**(3) Final Calculation for the Dataset:**

- Compute the average  $\Psi_s$  and  $\Delta_a$  for all trees in  $\Omega$ .
- Output the results for all trees in the dataset.

The structure sensitivity and abruptness of a topological index  $\mathcal{T}$  for a graph  $\mathcal{G}$  can be assessed through the following mathematical formulas:

To measure the structure sensitivity:

$$\Psi_s(\mathcal{T}, \mathcal{G}) = \frac{1}{|\mathcal{S}(\mathcal{G})|} \sum_{\mathcal{H} \in \mathcal{S}(\mathcal{G})} \left| \frac{\mathcal{T}(\mathcal{H}) - \mathcal{T}(\mathcal{G})}{\mathcal{T}(\mathcal{G})} \right|$$

And to capture the abruptness:

$$\Delta_a(\mathcal{T}, \mathcal{G}) = \max_{\mathcal{H} \in \mathcal{S}(\mathcal{G})} \left| \frac{\mathcal{T}(\mathcal{H}) - \mathcal{T}(\mathcal{G})}{\mathcal{T}(\mathcal{G})} \right|$$

In these equations,  $|\mathcal{S}(\mathcal{G})|$  denotes the total number of graphs within the set  $\mathcal{S}(\mathcal{G})$ . By calculating the average values of  $\Psi_s$  (structure sensitivity) and  $\Delta_a$  (abruptness) for a topological index  $\mathcal{T}$  across all graphs in a given class  $\Omega$ , we obtain the overall structure sensitivity and abruptness of  $\mathcal{T}$  for that class of connected graphs. Specifically,

$$\Psi_s(\mathcal{T}) = \frac{1}{|\Omega|} \sum_{\mathcal{G} \in \Omega} \Psi_s(\mathcal{T}, \mathcal{G})$$

and

$$\Delta_a(\mathcal{T}) = \frac{1}{|\Omega|} \sum_{\mathcal{G} \in \Omega} \Delta_a(\mathcal{T}, \mathcal{G})$$

where  $|\Omega|$  is the total number of graphs in the set  $\Omega$ . Numerous topological indices are mentioned in Table 1. Utilizing these (TIs) and definitions of sensitivity and abruptness, we generated the Table 2 for better understanding of applicability of Edge Moster index. We used the following algorithm to generate the mentioned tables.

---

**Algorithm 1** A MATLAB-based algorithm to compute structure sensitivity (SS) and abruptness (Abr) for topological indices (TIs) of a tree data set.

---

**Require:**  $\Omega = \{\text{Set of all trees with a given number of vertices}\}$

```

1:  $A \leftarrow \text{Zeros}(|\Omega|, 23)$ 
2:  $B \leftarrow \text{Zeros}(|\Omega|, 23)$ 
3:  $C \leftarrow \text{Zeros}(1, 23)$ 
4:  $D \leftarrow \text{Zeros}(1, 23)$ 
5: for  $i = 1$  to  $|\Omega|$  do ▷ For each tree  $T_i$  in  $\Omega$ 
6:    $S \leftarrow \{\text{Trees with GED} = 2 \text{ from } T_i\}$  ▷ GED computed using Python's networkx package
7:    $E \leftarrow [23 \text{ TIs for tree } T_i]_{1 \times 23}$  ▷ Step 1: Compute TIs for  $T_i$ 
8:    $F \leftarrow [23 \text{ TIs for trees in set } S]_{23 \times |S|}$  ▷ Step 2: Compute TIs for all trees in  $S$ 
9:    $G \leftarrow \text{Zeros}(23, |S|)$ 
10:   $H \leftarrow \text{Zeros}(1, 23)$ 
11:   $I \leftarrow \text{Zeros}(1, 23)$ 
12:  for  $j = 1$  to 23 do
13:     $p \leftarrow 0$ 
14:    for  $k = 1$  to  $|S|$  do
15:       $q \leftarrow \left| \frac{F(j,k) - E(j)}{E(j)} \right|$ 
16:       $G(j, k) \leftarrow q$ 
17:       $p \leftarrow p + q$ 
18:    end for
19:     $\text{SS}(T_i, \text{TIs}) \leftarrow \frac{p}{|S|}$  ▷ Step 3: Calculate structure sensitivity
20:     $\text{Abr}(T_i, \text{TIs}) \leftarrow \max(G(j, :))$  ▷ Step 3: Calculate abruptness
21:     $H(j) \leftarrow \text{SS}(T_i, \text{TIs})$  ▷ Store SS values for tree  $T_i$ 
22:     $I(j) \leftarrow \text{Abr}(T_i, \text{TIs})$  ▷ Store Abr values for tree  $T_i$ 
23:  end for
24:   $A(i, :) \leftarrow H(1, :)$ 
25:   $B(i, :) \leftarrow I(1, :)$ 
26: end for
27: Display:  $A, B$ 
28: for  $l = 1$  to 23 do
29:    $r \leftarrow 0, t \leftarrow 0$ 
30:   for  $m = 1$  to  $|\Omega|$  do
31:      $r \leftarrow A(l, m) + r$ 
32:      $t \leftarrow B(l, m) + t$ 
33:   end for
34:    $\text{SS}(\Omega, \text{TIs}) \leftarrow \frac{r}{|\Omega|}$ 
35:    $\text{Abr}(\Omega, \text{TIs}) \leftarrow \frac{t}{|\Omega|}$ 
36:    $C(l) \leftarrow \text{SS}(\Omega, \text{TIs})$ 
37:    $D(l) \leftarrow \text{Abr}(\Omega, \text{TIs})$ 
38: end for
39: Display:  $C, D$  ▷ Step 4: Output the average SS and Abr values for all TIs in  $\Omega$ 

```

---

Invariant	Symbol	Formula
First Zagreb Index	$M_1(G)$	$\sum_{v \in V(G)} d_G(v)^2 = \sum_{uv \in E(G)} (d_G(u) + d_G(v))$
Second Zagreb Index	$M_2(G)$	$\sum_{uv \in E(G)} d_G(u)d_G(v)$
Modified Second Zagreb	$mM_2(G)$	$\sum_{uv \in E(G)} \frac{1}{d_G(u)d_G(v)}$
Forgotten Index	$F(G)$	$\sum_{v \in V(G)} d_G(v)^3 = \sum_{uv \in E(G)} (d_G(u)^2 + d_G(v)^2)$
Randic Index	$R_{-1/2}(G)$	$\sum_{uv \in E(G)} \frac{1}{\sqrt{d_G(u)d_G(v)}}$
Reciprocal Randic Index	$RR_{-1/2}(G)$	$\sum_{uv \in E(G)} \sqrt{d_G(u)d_G(v)}$
Sum Connectivity Index	$SCI(G)$	$\sum_{uv \in E(G)} \frac{1}{\sqrt{d_G(u)+d_G(v)}}$
Symmetric Division Deg	$SDD(G)$	$\sum_{uv \in E(G)} \left( \frac{d_G(u)}{d_G(v)} + \frac{d_G(v)}{d_G(u)} \right)$
Harmonic Index	$H(G)$	$\sum_{uv \in E(G)} \frac{2}{d_G(u)+d_G(v)}$
Inverse Sum Index	$ISI(G)$	$\sum_{uv \in E(G)} \frac{d_G(u)d_G(v)}{d_G(u)+d_G(v)}$
Atom-Bond Connectivity	$ABC(G)$	$\sum_{uv \in E(G)} \frac{\sqrt{d_G(u)+d_G(v)-2}}{d_G(u)d_G(v)}$
Augmented Zagreb Index	$AZI(G)$	$\sum_{uv \in E(G)} \left( \frac{d_G(u)d_G(v)}{d_G(u)+d_G(v)-2} \right)^3$
First Hyper-Zagreb Index	$HM_1(G)$	$\sum_{uv \in E(G)} (d_G(u) + d_G(v))^2$
Second Hyper-Zagreb Index	$HM_2(G)$	$\sum_{uv \in E(G)} (d_G(u)d_G(v))^2$
Geometric-Arithmetic Index	$GA(G)$	$\sum_{uv \in E(G)} \frac{2\sqrt{d_G(u)d_G(v)}}{d_G(u)+d_G(v)}$
Arithmetic-Geometric Index	$AG(G)$	$\sum_{uv \in E(G)} \frac{d_G(u)+d_G(v)}{2\sqrt{d_G(u)d_G(v)}}$
Sombor Index	$SO(G)$	$\sum_{uv \in E(G)} \sqrt{d_G(u)^2 + d_G(v)^2}$
Modified Sombor Index	$mSO(G)$	$\sum_{uv \in E(G)} \frac{1}{\sqrt{d_G(u)^2 + d_G(v)^2}}$
Nirmala Index	$N(G)$	$\sum_{uv \in E(G)} \sqrt{d_G(u) + d_G(v)}$
First Inverse Nirmala Index	$IN_1(G)$	$\sum_{uv \in E(G)} \sqrt{\frac{1}{d_G(u)} + \frac{1}{d_G(v)}}$
Second Inverse Nirmala Index	$IN_2(G)$	$\sum_{uv \in E(G)} \frac{1}{\sqrt{\frac{1}{d_G(u)} + \frac{1}{d_G(v)}}$
Geometric-Quadratic Index	$GQ(G)$	$\sum_{uv \in E(G)} \frac{\sqrt{2d_G(u)d_G(v)}}{\sqrt{d_G(u)^2 + d_G(v)^2}}$
Quadratic-Geometric Index	$QG(G)$	$\sum_{uv \in E(G)} \frac{\sqrt{d_G(u)^2 + d_G(v)^2}}{\sqrt{2d_G(u)d_G(v)}}$

**Table 1.** Topological indices with their symbols and formulas

Descriptors	Parameters	$n = 4$	$n = 5$	$n = 6$	$n = 7$	$n = 8$	$n = 9$	$n = 10$
SO	Sensitivity	0.2691	0.2398	0.1864	0.1595	0.1263	0.1101	0.0939
	Abruptness	0.2667	0.2762	0.2781	0.2901	0.2394	0.2228	0.2091
$RR_{-1/2}$	Sensitivity	0.0754	0.0813	0.0707	0.0631	0.0587	0.0501	0.0447
	Abruptness	0.0722	0.0854	0.1011	0.7198	0.1372	0.1087	0.1078
G Q	Sensitivity	0.1857	0.1676	0.1243	0.0978	0.0767	0.0632	0.0531
	Abruptness	0.1851	0.1805	0.1721	0.1456	0.1309	0.1177	0.1056
$HM_1$	Sensitivity	0.3562	0.3509	0.2809	0.2391	0.2041	0.1809	0.1596
	Abruptness	0.3534	0.3956	0.4333	0.4194	0.4029	0.3922	0.3799
A G	Sensitivity	0.1061	0.0982	0.0745	0.0613	0.0496	0.0426	0.0355
	Abruptness	0.1068	0.1103	0.1099	0.0984	0.0892	0.0829	0.0749
$^m$ SO	Sensitivity	0.2795	0.2652	0.2039	0.0103	0.1289	0.1062	0.0882
	Abruptness	0.2814	0.2826	0.2794	0.2427	0.2225	0.1999	0.1797
$IN_2$	Sensitivity	0.0142	0.0121	0.0105	0.0221	0.0107	0.0093	0.0089
	Abruptness	0.0140	0.0144	0.0155	0.0967	0.0193	0.0207	0.0228
ISI	Sensitivity	0.0381	0.0320	0.0302	0.0286	0.0274	0.0257	0.0248
	Abruptness	0.0373	0.0385	0.0427	0.0482	0.0549	0.0584	0.0619
F	Sensitivity	0.5388	0.4899	0.3691	0.3077	0.2565	0.2243	0.1937
	Abruptness	0.5376	0.5669	0.5959	0.5572	0.5188	0.4912	0.4706
SDD	Sensitivity	0.3685	0.3191	0.2395	0.1957	0.1578	0.1343	0.1157
	Abruptness	0.3663	0.3688	0.3693	0.3302	0.3029	0.2809	0.2607
$IN_1$	Sensitivity	0.0051	0.0042	0.0037	0.0035	0.0033	0.0029	0.0028
	Abruptness	0.0045	0.0043	0.0047	0.0053	0.0057	0.0061	0.0164
$^mM_2$	Sensitivity	0.2283	0.2137	0.1645	0.1301	0.1027	0.0839	0.0692
	Abruptness	0.2281	0.2342	0.2267	0.1998	0.1769	0.1601	0.1444
N	Sensitivity	0.0954	0.0923	0.0715	0.0595	0.0493	0.0426	0.0367
	Abruptness	0.0957	0.1014	0.1049	0.0974	0.0902	0.0845	0.0794
$QG$	Sensitivity	0.1824	0.1613	0.1199	0.0967	0.0779	0.0663	0.0556
	Abruptness	0.1823	0.1808	0.1774	0.1576	0.1425	0.1307	0.1198
$Mo_eG$	Sensitivity	0.1217	0.2548	0.3182	0.3217	0.3209	0.3032	0.2883
	Abruptness	0.0049	0.0045	0.0049	0.0055	0.0059	0.0064	0.0069

**Table 2.** Topological indices with their sensitivity and abruptness

For evaluating the quality of a topological index, it is crucial that the structural sensitivity ( $\Psi_s$ ) is maximized, while the abruptness ( $\Delta_a$ ) is minimized. More details on these two measures are explored in [37, 38], where computational testing of the smoothness of several distance- and degree-based indices was examined using data sets of trees with varying vertex counts. Table 2 leads to the following observations: the neighborhood face index, forgotten index, and first hyper-Zagreb index exhibit the highest, second-highest, and third-highest  $\Psi_s$  values, respectively. From Tables 2, we see for trees with  $n = 10$  vertices that  $\Psi_s(Mo_eG) = 0.288$ ,  $\Psi_s(F) = 0.192$ , and  $\Psi_s(\mathcal{H}\mathcal{M}_1) = 0.157$ , followed by  $\Psi_s(\mathcal{A}\mathcal{L}\mathcal{I}) = 0.118$ ,  $\Psi_s(\mathcal{S}\mathcal{D}\mathcal{D}) = 0.112$ ,  $\Psi_s(\mathcal{M}_2) = 0.103$ ,  $\Psi_s(\mathcal{S}\mathcal{O}) = 0.093$ ,  $\Psi_s({}^m\mathcal{S}\mathcal{O}) = 0.086$ ,  $\Psi_s(\mathcal{M}_1) = 0.073$ ,  $\Psi_s({}^m\mathcal{M}_2) = 0.067$ , and  $\Psi_s(H) = 0.067$ , among others. These invariants maintain the following relationship:

$$\begin{aligned} \Psi_s(Mo_eG) &> \Psi_s(F) > \Psi_s(\mathcal{H}\mathcal{M}_1) > \Psi_s(\mathcal{A}\mathcal{L}\mathcal{I}) > \Psi_s(\mathcal{S}\mathcal{D}\mathcal{D}) > \Psi_s(\mathcal{M}_2) > \Psi_s(\mathcal{G}\mathcal{L}) \\ &> \Psi_s(\mathcal{S}\mathcal{O}) > \Psi_s({}^m\mathcal{S}\mathcal{O}) > \Psi_s(\mathcal{M}_1) > \Psi_s({}^m\mathcal{M}_2) > \Psi_s(H) > \Psi_s(\mathcal{Q}\mathcal{G}) \\ &> \Psi_s(\mathcal{R}\mathcal{R}_{-1/2}) > \Psi_s(N) > \Psi_s(\mathcal{S}\mathcal{C}\mathcal{I}) > \Psi_s(\mathcal{R}_{-1/2}) \approx \Psi_s(\mathcal{A}\mathcal{G}) > \Psi_s(\mathcal{G}\mathcal{A}) \\ &> \Psi_s(\mathcal{A}\mathcal{B}\mathcal{C}) > \Psi_s(\mathcal{I}\mathcal{I}\mathcal{I}) > \Psi_s(\mathcal{I}\mathcal{N}_2) > \Psi_s(\mathcal{I}\mathcal{N}_1) \end{aligned}$$

On the other hand, the topological indices with the lowest abruptness ( $\Delta_a$ ) are the ( $Mo_eG$ ) and the first and second inverse Nirmala indices. For  $n = 10$ , Table 2 show that  $\Delta_a(Mo_eG) = 0.005$ ,  $\Delta_a(\mathcal{I}\mathcal{N}_2) = 0.021$ , followed by  $\Delta_a(\mathcal{A}\mathcal{B}\mathcal{C}) = 0.057$ ,  $\Delta_a(\mathcal{I}\mathcal{I}\mathcal{I}) = 0.0604$ ,  $\Delta_a(\mathcal{G}\mathcal{A}) = 0.0671$ ,  $\Delta_a(\mathcal{R}_{-1/2}) = 0.071$ , and  $\Delta_a(\mathcal{S}\mathcal{C}\mathcal{I}) = 0.0714$ , among others. The following inequality relation holds for the degree-based indices:

$$\begin{aligned} \Delta_a(Mo_eG) &< \Delta_a(\mathcal{I}\mathcal{N}_1) < \Delta_a(\mathcal{I}\mathcal{N}_2) < \Delta_a(\mathcal{A}\mathcal{B}\mathcal{C}) < \Delta_a(\mathcal{I}\mathcal{I}\mathcal{I}) < \Delta_a(\mathcal{G}\mathcal{A}) < \Delta_a(\mathcal{R}_{-1/2}) \\ &< \Delta_a(\mathcal{S}\mathcal{C}\mathcal{I}) < \Delta_a(\mathcal{A}\mathcal{G}) < \Delta_a(N) < \Delta_a(\mathcal{R}\mathcal{R}_{-1/2}) < \Delta_a(\mathcal{G}\mathcal{L}) < \Delta_a(\mathcal{Q}\mathcal{G}) \\ &< \Delta_a(H) < \Delta_a({}^m\mathcal{M}_2) < \Delta_a(\mathcal{M}_1) < \Delta_a({}^m\mathcal{S}\mathcal{O}) < \Delta_a(\mathcal{A}\mathcal{L}\mathcal{I}) \\ &< \Delta_a(\mathcal{S}\mathcal{D}\mathcal{D}) < \Delta_a(\mathcal{M}_2) < \Delta_a(\mathcal{H}\mathcal{M}_1) < \Delta_a(F) < \Delta_a(\mathcal{H}\mathcal{M}_2) \end{aligned}$$

Above sensitivity analysis depicts to assess how stable Mostar and edge version of Mostar index are when small changes, such as adding or removing edges or nodes, occur in the graph.

### 3. REGRESSION ANALYSIS

We collected data on 13 tuberculosis (TB) drugs and their six physicochemical properties from reputable online sources like PubChem and ChemSpider. Subsequently, we calculated the numerical results of ten degree-based reducible indices to analyze the molecular structure of these drugs using three techniques: edge partition, vertex degree, and counting degree. We employed Quantitative Structure-Activity Relationship (QSAR) analysis to establish a strong positive correlation between the indices and properties, utilizing linear, quadratic, and logarithmic regression equations for this purpose. The correlation coefficient ( $r$ ) was one of the statistical parameters employed to assess the reliability and significance of the relationship between the physical properties and calculated numerical values of the TB drugs. Finally, we created line graphs to visually compare the correlation coefficients, facilitating a comprehensive discussion of the relationships between the properties and indices. The physicochemical parameters of the specified pharmaceuticals are outlined in Table 3, which provides exact values for the molar index, whereas experimental values for molar mass, XLOGP3, complexity, LOGP, melting temperature, and collision cross section were gathered from the PubChem website. We evaluated the regression models for mentioned descriptor utilizing the data supplied in Table 3 and investigated its chemical applicability.

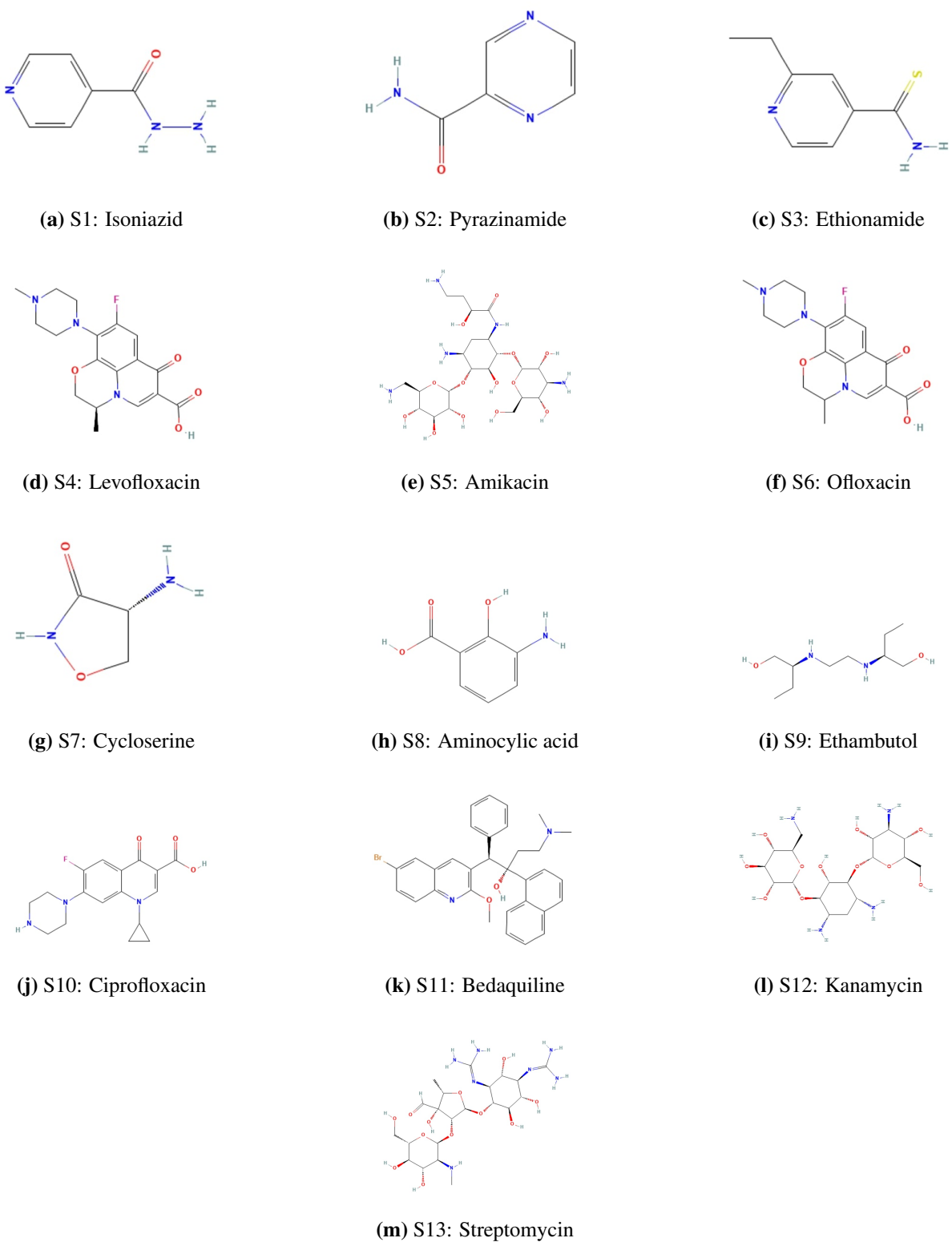


**Figure 1.** Comparison of anti-tuberculosis drugs categorized by their respective subfigures (S1–S13), showcasing a visual representation of each drug for analysis and reference

Medicine Name	$Mo_eG$	$MM$	$XLOGP3$	$C$	$LOGP$	$MP$	$CCS$
Isoniazid	48	137.14	-0.7	120	-0.7	340.5	125.6
Pyrazinamide	35	123.11	-0.6	115	-0.6	376	122.8
Ethionamide	57	166.25	1.1	147	0.5	327	135.8
Levofloxacin	394	361.4	-0.4	634	0.32	225	188.5
Amikacin	1107	585.6	-7.9	819	-8.78	240	235.1
Ofloxacin	394	361.4	-0.4	634	-0.39	254	188.5
Cycloserine	20	102.09	-1.5	929	0	155.5	97
4-aminosalicylic acid	55	153.14	1.3	160	0.89	150.5	138
Ethambutol	100	204.31	-0.1	109	0.4	171.5	170
Ciprofloxacin	346	331.34	-1.1	571	0.28	255	185.3
Bedaquiline	1123	555.5	7.2	715	7.74	118	205
Kanamycin	657	484.5	-6.9	638	-6.3	57	206.6
Streptomycin	1154	581.6	-8	940	-2.53	230	231

**Table 3.** Mostar index and physical properties for each medicine.

### 3.1. Step 1: Compute Correlation Coefficient $R$ .

The formula for the correlation coefficient  $R$  is:

$$(3) \quad R = \frac{n \sum xy - \sum x \sum y}{\sqrt{[n \sum x^2 - (\sum x)^2] [n \sum y^2 - (\sum y)^2]}}$$

Where:

- $x$  represents the independent variable (e.g.,  $MM$ )
- $y$  represents the dependent variable  $Mo(G)$
- $n$  is the number of data points.

### 3.2. Step 2: Compute the Regression Coefficients.

The linear regression equation is of the form:

$$(4) \quad Mo(G) = \beta_0 + \beta_1 \times MM$$

Where:

- $\beta_0$  is the intercept.
- $\beta_1$  is the slope, computed as:

$$(5) \quad \beta_1 = \frac{n \sum xy - \sum x \sum y}{n \sum x^2 - (\sum x)^2}$$

And the intercept  $\beta_0$  is:

$$(6) \quad \beta_0 = \frac{\sum y - \beta_1 \sum x}{n}$$

**3.3. Step 3: Compute  $R^2$ .** Once you have  $\beta_0$  and  $\beta_1$ , compute  $R^2$ , the coefficient of determination, as follows:

$$(7) \quad R^2 = 1 - \frac{\sum (y_i - \hat{y}_i)^2}{\sum (y_i - \bar{y})^2}$$

Where:

- $\hat{y}_i$  is the predicted value from the regression model.
- $y_i$  is the observed value.
- $\bar{y}$  is the mean of the dependent variable.

**3.4. Step 4: Compute Standard Error of Estimation (SEE).** The formula for SEE is:

$$(8) \quad SEE = \sqrt{\frac{\sum (y_i - \hat{y}_i)^2}{n - 2}}$$

**3.5. Step 5: Compute Fisher Ratio  $F$ .** The  $F$ -value is computed as:

$$(9) \quad F = \frac{R^2}{(1 - R^2)} \times \frac{n - 2}{1}$$

**3.6. Step 6: Apply the Formulas to the Data.** In this subsection, we manually compute these statistical quantities for  $Mo(G)$  and  $MM$ . Let's first calculate the sums and sums of squares necessary for the correlation and regression calculations. For the independent variable  $MM$ , here are the manually calculated results:

- Linear Regression Model:  $Mo(G) = -326.04 + 2.35 \times MM$
- Correlation Coefficient  $R$ : 0.973
- Adjusted Coefficient of Determination  $R^2$ : 0.946
- Standard Error of Estimation (SEE): 107.93
- Fisher Ratio  $F$ : 193.45

This process can be repeated for the other variables ( $XLOGP3$ ,  $C$ ,  $LOGP$ ,  $MP$ , and  $CCS$ ) by following the same steps. Hence Table 4 is generated.

<i>Chemical Properties</i>	<i>R</i>	<i>R<sup>2</sup><sub>adj</sub></i>	<i>SEE</i>	<i>F</i>	<i>Linear Regression Model</i>
MM	0.973	0.941	107.93	193.45	$M_{e}o(G) = -326.04 + 2.35 \times \text{MM}$
XLOGP3	0.336	0.032	438.33	1.40	$M_{e}o(G) = 372.63 - 35.88 \times \text{XLOGP3}$
C	0.695	0.436	334.67	10.27	$M_{e}o(G) = -55.48 + 0.95 \times \text{C}$
LOGP	0.198	-0.048	456.15	0.45	$M_{e}o(G) = 406.22 - 22.80 \times \text{LOGP}$
MP	0.991	0.990	436.61	1.49	$M_{o}(G) = 796.27 - 1.68 \times \text{MP}$
CCS	0.889	0.771	213.34	41.33	$M_{e}o(G) = -1123.96 + 9.02 \times \text{CCS}$

**Table 4.** Mostar index and physical properties for each medicine.

The Edge Mostar index ( $M_{e}o(G)$ ) serves as a valuable predictor for various chemical properties, with linear regression analysis revealing its effectiveness in modeling relationships with melting point (MP), molecular mass (MM), and other characteristics. Among the six properties examined (MM, XLOGP3, C, LOGP, MP, and CCS), MP stands out with the strongest correlation coefficient ( $R = 0.991$ ) and an exceptionally high adjusted  $R^2$  value of 0.990. These results indicate that  $M_{o}(G)$  can reliably predict MP, capturing nearly all its variation. The low standard error of estimation ( $SEE = 107.93$ ) underscores the precision of these predictions, and the significant Fisher ratio ( $F = 193.45$ ) further validates the robustness of the regression model for MP. Similarly,  $M_{o}(G)$  demonstrates strong predictive capability for molecular mass (MM), with a correlation coefficient of  $R = 0.973$  and an adjusted  $R^2$  value of 0.941. These metrics suggest that MM is also well-modeled by the Mostar index. The small SEE value of 107.93 indicates that predictions based on  $M_{o}(G)$  are close to the actual values of MM. This highlights the index's reliability in predicting properties tied to molecular size and weight.

In contrast, the predictive power of  $M_{o}(G)$  diminishes for properties such as XLOGP3, LOGP, and carbon count (C). XLOGP3 and LOGP exhibit weak correlations, with  $R$  values of 0.336 and 0.198, respectively, and adjusted  $R^2$  values close to zero or negative. These results suggest that  $M_{o}(G)$  is a poor predictor for properties related to hydrophobicity. The high SEE values (438.33 for XLOGP3 and 456.15 for LOGP) further indicate substantial errors in prediction, making these properties less suitable for linear regression models based on  $M_{o}(G)$ . Similarly, the carbon count (C) shows limited predictive value, reflecting a weak relationship with  $M_{o}(G)$ . The CCS property, however, presents a moderate correlation with  $M_{o}(G)$ , with

$R = 0.889$  and an adjusted  $R^2$  value of 0.771. While not as strong as MP or MM, CCS demonstrates that the Mostar index can reasonably predict structural attributes related to this property. The SEE value of 213.34 suggests moderate prediction accuracy, positioning CCS as a property with potential for further investigation. Overall, these findings establish  $Mo(G)$  as a significant predictor for certain chemical properties, particularly MP and MM, where the index demonstrates strong linear relationships and high predictive accuracy. While its utility is limited for properties like XLOGP3, LOGP, and C,  $Mo(G)$  shows potential for moderate prediction of CCS. This analysis underscores the versatility of graph-theoretical indices in chemical property prediction and highlights areas for refinement and future exploration.

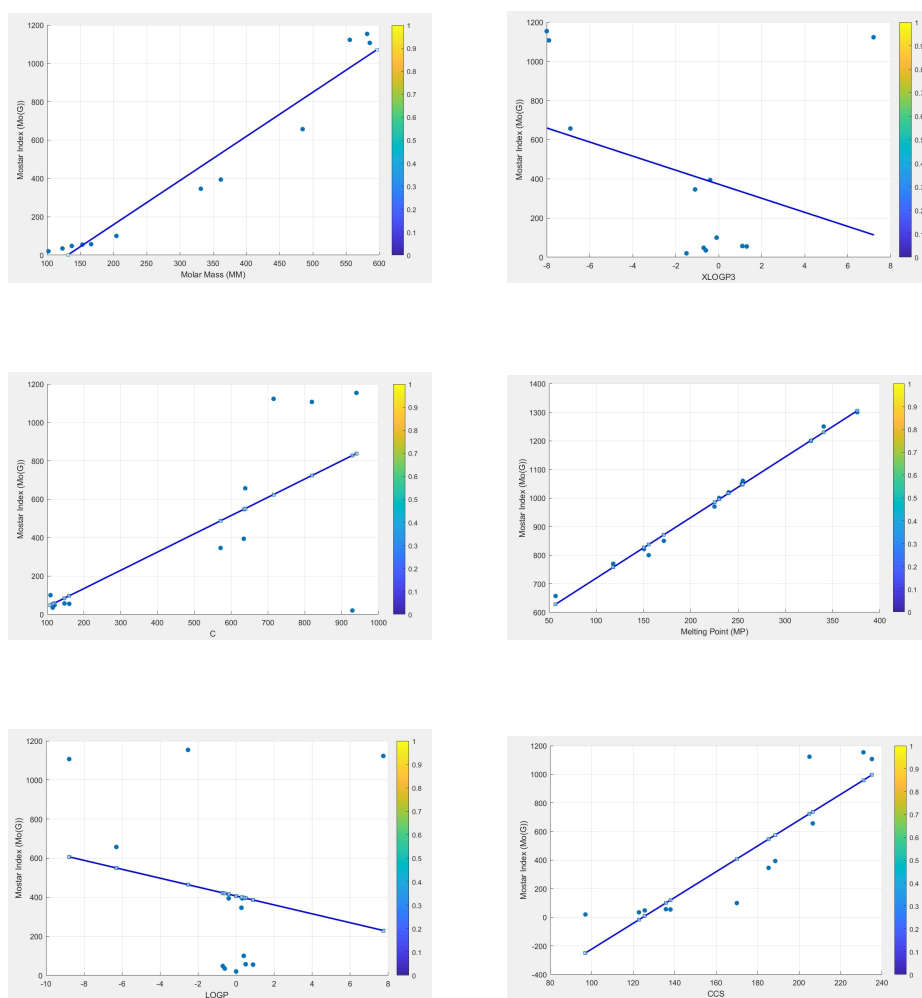


**Figure 2.** Comparative representation of numeric values evaluated in Table 1 & 2 for Generalized mesh network graph ( $\mathcal{M}_m^n$ ) with  $m$  set to 2, where  $2 \leq n \leq 15$

#### **4. CONCLUSION**

This study has conducted a comprehensive examination of essential anti-tuberculosis medications, including Isoniazid, Levofloxacin, Cycloserine, Ciprofloxacin, Pyrazinamide, Amikacin, 4-Aminosalicylic Acid, Bedaquiline, Streptomycin, Ethionamide, Ofloxacin, Ethambutol, and Kanamycin. The structural sensitivity investigation validated the relevance of the Edge Mostar topological invariant for these pharmaceuticals, demonstrating optimal sensitivity and low abruptness. The QSPR research indicated that the Mostar index has a robust association with significant physicochemical parameters, including melting point (with correlation  $> 0.990$ ) and molar mass (correlation  $> 0.970$ ). The results demonstrate that the Edge Mostar index is a very dependable predictor of the physicochemical qualities of pharmaceuticals utilized in the treatment of diseases such as tuberculosis. This discovery could greatly facilitate the creation of innovative therapeutic agents by utilizing the predictive capabilities of the Mostar index for pharmacological characteristics.

#### **ACKNOWLEDGMENT**

This article has been produced with the financial support of the European Union under the REFRESH – Research Excellence For Region Sustainability and High-tech Industries project number CZ.10.03.01/00/22\_003/0000048 via the Operational Programme Just Transition.

#### **AVAILABILITY OF DATA AND MATERIALS**

The data is provided on request to the authors.

#### **AUTHORS' CONTRIBUTION**

All authors contributed equally in writing of this article.

#### **CONFLICT OF INTERESTS**

The authors declare that there is no conflict of interests.

**REFERENCES**

- [1] World Health Organization, Global Tuberculosis Report 2021, WHO, 2021. <https://www.who.int/publications/i/item/9789240037021>.
- [2] V. Kumar, A.K. Abbas, J.C. Aster, J.A. Perkins, eds., Robbins Basic Pathology, Elsevier, 2018.
- [3] P. Nahid, S.E. Dorman, N. Alipanah, et al. Official American Thoracic Society/Centers for Disease Control and Prevention/Infectious Diseases Society of America Clinical Practice Guidelines: Treatment of Drug-Susceptible Tuberculosis, *Clin. Infect. Dis.* 63 (2016), e147–e195. <https://doi.org/10.1093/cid/ciw376>.
- [4] N. Ali, Z. Kousar, M. Safdar, et al. Mapping Connectivity Patterns: Degree-Based Topological Indices of Corona Product Graphs, *J. Appl. Math.* 2023 (2023), 8975497. <https://doi.org/10.1155/2023/8975497>.
- [5] M.L.S. Bhanu, M.P. Kumari, T. Begum M, Anti-Tuberculosis Drugs and Mechanisms of Action: Review, *Int. J. Infect. Dis. Res.* 4 (2023), 1–7.
- [6] P. Prasanna, S. Rathee, A. Upadhyay, S. Sulakshana, Nanotherapeutics in the Treatment of Acute Respiratory Distress Syndrome, *Life Sci.* 276 (2021), 119428. <https://doi.org/10.1016/j.lfs.2021.119428>.
- [7] R.S. Mitchell, Present-Day Management of Tuberculosis, *J. Chronic Dis.* 4 (1956), 607–634. [https://doi.org/10.1016/0021-9681\(56\)90051-0](https://doi.org/10.1016/0021-9681(56)90051-0).
- [8] A. Jain, R. Kumar, P. Mothsra, A.K. Sharma, A.K. Singh, Y. Kumar, Recent Biochemical Advances in Antitubercular Drugs: Challenges and Future, *Curr. Topics Med. Chem.* 24 (2024), 1829–1855. <https://doi.org/10.2174/0115680266286294240610102911>.
- [9] S. Janssen, M. Murphy, C. Upton, B. Allwood, A.H. Diacon, Tuberculosis: An Update for the Clinician, *Respirology* 30 (2025), 196–205. <https://doi.org/10.1111/resp.14887>.
- [10] E. Pontali, G. Sotgiu, L. D’Ambrosio, R. Centis, G.B. Migliori, Bedaquiline and Multidrug-Resistant Tuberculosis: A Systematic and Critical Analysis of the Evidence, *Eur. Respir. J.* 47 (2016), 394–402. <https://doi.org/10.1183/13993003.01891-2015>.
- [11] B. Almutairy, Extensively and Multidrug-Resistant Bacterial Strains: Case Studies of Antibiotics Resistance, *Front. Microbiol.* 15 (2024), 1381511. <https://doi.org/10.3389/fmicb.2024.1381511>.
- [12] H.K. Agibothu Kupparam, I. Shah, P. Chandrasekaran, et al. Pharmacokinetics of Anti-TB Drugs in Children and Adolescents with Drug-Resistant TB: A Multicentre Observational Study from India, *J. Antimicrob. Chemother.* 79 (2024), 2939–2947. <https://doi.org/10.1093/jac/dkae311>.
- [13] J. Wang, Y. Ma, X. Zhou, et al. Integrated Ecological-Health Risk Assessment of Ofloxacin, *J. Hazard. Mater.* 487 (2025), 137178. <https://doi.org/10.1016/j.jhazmat.2025.137178>.
- [14] A. Tabassum, M.A. Javed, S. Shahzad, Tuberculosis; Nanotechnology-Revolutionized Prevention & Treatment Strategies, *Continental Vet. J.* 4 (2024), 132–145. <https://doi.org/10.71081/cvj/2024.024>.

- [15] A. Raza, M. Ismaeel, F.T. Tolasa, Valency Based Novel Quantitative Structure Property Relationship (QSPR) Approach for Predicting Physical Properties of Polycyclic Chemical Compounds, *Sci. Rep.* 14 (2024), 7080. <https://doi.org/10.1038/s41598-024-54962-5>.
- [16] A. Raza, M.M. Munir, Exploring Spectrum-Based Descriptors in Pharmacological Traits through Quantitative Structure Property (QSPR) Analysis, *Front. Phys.* 12 (2024), 1348407. <https://doi.org/10.3389/fphy.2024.1348407>.
- [17] J. Wei, A. Fahad, A. Raza, P. Shabir, A. Alameri, On Distance Dependent Entropy Measures of Poly Propylene Imine and Zinc Porphyrin Dendrimers, *Int. J. Quantum Chem.* 124 (2024), e27322. <https://doi.org/10.1002/qua.27322>.
- [18] D. Alghazzawi, A. Raza, U. Munir, Md.S. Ali, Chemical Applicability of Newly Introduced Topological Invariants and Their Relation with Polycyclic Compounds, *J. Math.* 2022 (2022), 5867040. <https://doi.org/10.1155/2022/5867040>.
- [19] T.D. Rakhmatovna, Prevalence of Extensively Drug-Resistant Tuberculosis, *J. Human. Nat. Sci.* 17 (2024), 117–121.
- [20] H. Wiener, Structural Determination of Paraffin Boiling Points, *J. Amer. Chem. Soc.* 69 (1947), 17–20. <https://doi.org/10.1021/ja01193a005>.
- [21] H. Wiener, Correlation of Heats of Isomerization, and Differences in Heats of Vaporization of Isomers, Among the Paraffin Hydrocarbons, *J. Amer. Chem. Soc.* 69 (1947), 2636–2638. <https://doi.org/10.1021/ja01203a022>.
- [22] M.O. Albertson, The Irregularity of a Graph, *Ars. Comb.* 46 (1997), 219–225.
- [23] T. Reti, R. Sharfdini, A. Dregelyi-kiss, et al. Graph Irregularity Indices Used as Molecular Descriptors on QSPR Studies, *MATCH. Commun. Math. Comput. Chem.* 79 (2018), 509–524.
- [24] V.R. Kulli, On K Banhatti Indices of Graphs, *J. Comput. Math. Sci.* 7 (2016), 213–218.
- [25] J. Zheng, Z. Iqbal, A. Fahad, et al. Some Eccentricity-Based Topological Indices and Polynomials of Poly(ETHyleneAmidoAmine) (PETAA) Dendrimers, *Processes* 7 (2019), 433. <https://doi.org/10.3390/pr7070433>.
- [26] A. Fahad, M.I. Qureshi, S. Noureen, et al. Topological Descriptors of Poly Propyl Ether Imine (PETIM) Dendrimers, *Biointerface Res. Appl. Chem.* 11 (2020), 10968–10978. <https://doi.org/10.33263/BRIAC113.1096810978>.
- [27] Zagreb Connection Index of Drugs Related Chemical Structures, *Biointerface Res. Appl. Chem.* 11 (2020), 11920–11930. <https://doi.org/10.33263/BRIAC114.1192011930>.
- [28] Y.-M. Chu, M. Abid, M.I. Qureshi, A. Fahad, A. Aslam, Irregular Topological Indices of Certain Metal Organic Frameworks, *Main Group Metal Chem.* 44 (2021), 73–81. <https://doi.org/10.1515/mgmc-2021-0009>.

- [29] T. Došlić, I. Martinjak, R. Škrekovski, et al. Mostar Index, *J. Math. Chem.* 56 (2018), 2995–3013. <https://doi.org/10.1007/s10910-018-0928-z>.
- [30] K. Deng, S. Li, Extremal Catacondensed Benzenoids with Respect to the Mostar Index, *J. Math. Chem.* 58 (2020), 1437–1465. <https://doi.org/10.1007/s10910-020-01135-0>.
- [31] A. Tepeh, Extremal Bicyclic Graphs with Respect to Mostar Index, *Appl. Math. Comput.* 355 (2019), 319–324. <https://doi.org/10.1016/j.amc.2019.03.014>.
- [32] N. Tratnik, Computing the Mostar Index in Networks with Applications to Molecular Graphs, *Iran. J. Math. Chem.* 12 (2021), 1–18. <https://doi.org/10.22052/IJMC.2020.240316.1526>.
- [33] M. Arockiaraj, J. Clement, N. Tratnik, Mostar Indices of Carbon Nanostructures and Circumscribed Donut Benzenoid Systems, *Int. J. Quantum Chem.* 119 (2019), e26043. <https://doi.org/10.1002/qua.26043>.
- [34] M. Arockiaraj, J. Clement, N. Tratnik, S. Mushtaq, K. Balasubramanian, Weighted Mostar Indices as Measures of Molecular Peripheral Shapes with Applications to Graphene, Graphyne and Graphdiyne Nanoribbons, *SAR QSAR Environ. Res.* 31 (2020), 187–208. <https://doi.org/10.1080/1062936X.2019.1708459>.
- [35] F. Hayat, B. Zhou, On Cacti with Large Mostar Index, *Filomat* 33 (2019), 4865–4873. <https://doi.org/10.2298/FIL1915865H>.
- [36] B. Furtula, I. Gutman, M. Dehmer, On Structure-Sensitivity of Degree-Based Topological Indices, *Appl. Math. Comput.* 219 (2013), 8973–8978. <https://doi.org/10.1016/j.amc.2013.03.072>.
- [37] I. Redžepović, B. Furtula, Comparative Study on Structural Sensitivity of Eigenvalue-Based Molecular Descriptors, *J. Math. Chem.* 59 (2021), 476–487. <https://doi.org/10.1007/s10910-020-01202-6>.
- [38] K. Zemljič, P. Žigert Pleteršek, Smoothness of Graph Energy in Chemical Graphs, *Mathematics* 11 (2023), 552. <https://doi.org/10.3390/math11030552>.